JOURNAL OF VIROLOGY, May 2011, p. 4937–4946 Vol. 85, No. 10
0022-538X/11/$12.00 doi:10.1128/JVI.02358-10

Identification of a Human SCARB2 Region That Is Important for Enterovirus 71 Binding and Infection▽

Seiya Yamayoshi and Satoshi Koike*

Neurovirology Project, Tokyo Metropolitan Institute of Medical Science, Tokyo Metropolitan Organization for Medical Research, 2-1-6, Kamikitazawa, Setagaya-ku, Tokyo 156-8506, Japan

Received 10 November 2010/Accepted 28 February 2011

We previously identified human scavenger receptor class B, member 2 (SCARB2), as a cellular receptor for enterovirus 71 (EV71). Expression of human SCARB2 (hSCARB2) permitted mouse L929 cells to efficiently bind to virions and to produce both viral proteins and progeny viruses upon EV71 infection. Mouse Scarb2 (mScarb2) exhibited 85.8% amino acid identity and 99.9% similarity to hSCARB2. The expression of mScarb2 in L929 cells conferred partial susceptibility. Very few virions bound to mScarb2-expressing cells. The viral titer in L929 cells expressing mScarb2 was approximately 40- to 100-fold lower than that in L929 cells expressing hSCARB2. Using hSCARB2–mScarb2 chimeric mutants, we attempted to map the region that was important for efficient EV71 infection. L929 cells expressing chimeras that carried amino acids 142 to 204 from the human sequence were susceptible to EV71, while chimeras that carried the mouse sequence in this region were not. Moreover, this region was also critical for binding to virions. The determination of this region in hSCARB2 that is important for EV71 binding and infection greatly contributes to the understanding of virus-receptor interactions. Further studies will clarify the early steps of EV71 infection.

Enterovirus 71 (EV71), together with coxsackievirus A16 (CVA16), belongs to human enterovirus species A of the genus *Enterovirus* within the family *Picornaviridae* (28). The virus contains a single-stranded, positive-sense RNA surrounded by an icosahedral capsid assembled from 60 copies of each of the four structural proteins: VP1, VP2, VP3, and VP4 (32). EV71 was first isolated from patients with neurological diseases, including fatal encephalitis and aseptic meningitis, in California from 1969 to 1972 (33). Later studies revealed that EV71 is associated with hand-foot-and-mouth disease (HFMD) in young children and infants (6, 13). Although HFMD is generally considered a mildly infectious disease, HFMD caused by EV71, but not by other enteroviruses, is sometimes involved with severe neurological diseases, including brain stem encephalitis and acute flaccid paralysis (23). In recent years, epidemic or sporadic outbreaks of neurovirulent EV71 infections have been reported mainly in Southeast or East Asia, including Taiwan, Malaysia, Singapore, Japan, and China (1, 8, 11, 17, 27, 38). In particular, the epidemic outbreaks that occurred in 2008 and 2009 in China resulted in a total of 488,955 and 1,155,525 HFMD cases, including 126 and 353 fatal cases per year, respectively (http://www.moh.gov.cn/publicfiles/business/htmlfiles/mohbgt/s3582/201002/46043.htm) (40). Moreover, the EV71 epidemic has since continued in China, with 987,779 HFMD cases, including 537 fatal cases reported as of 22 June 2010 (http://www.moh.gov.cn/publicfiles/business/htmlfiles/mohbgt/s3582/201006/47871.htm).

Human RD cells are highly susceptible to EV71 infection, whereas mouse L929 cells exhibit very low susceptibility. We previously reported the identification of EV71 receptors by genetic complementation of L929 cells with genes transferred from human RD cells (37). Briefly, we established two EV71-susceptible cell lines that carried a portion of human genomic DNA. By identifying the integrated human DNA in one of the transformants, Ltr051 cells, we have shown that scavenger receptor class B, member 2 (SCARB2), is a cellular receptor for EV71. SCARB2 serves as a receptor for all EV71 isolates tested. EV71 infection in the SCARB2-expressing L929 cell line is as efficient as that in the RD cell line (37). We have also found that virus replication efficiency in another transformant cell line, Ltr246, is slightly lower than that in Ltr051 cells (37) and that Ltr246 cells are susceptible to only a subset of EV71 strains (S. Yamayoshi et al., unpublished data). Although Ltr246 cells appear to express another, unknown receptor (receptor X), we have not yet identified the human DNA sequence that confers susceptibility on Ltr246 cells. In addition, Nishimura et al. also have identified the selectin P ligand (SELPLG, also known as P-selectin glycoprotein ligand-1 [PSGL-1]) as an EV71 receptor from human T cell leukemia Jurkat cells by using the panning assay, which enriched for molecules with strong binding affinity to EV71 particles (26). SELPLG also confers susceptibility only to some EV71 strains on L929 cells. In Jurkat cells and L929 cells expressing SELPLG, however, the appearance of cytopathic effect (CPE) and the expression of viral proteins after EV71 infection occurred more slowly than in RD cells and L929 cells expressing SCARB2 (26). We have confirmed that Ltr246 cells do not carry the human *SCARB2* and *SELPLG* genes. Another study has shown that the depletion of O-linked glycans or pretreatment with sialidase reduced EV71 infection in DLD-1 human colon cancer cells (39). These results suggest that EV71 can enter the cell via multiple pathways. Because all EV71 strains tested used SCARB2 as the receptor (37), whereas only a subset of EV71 strains used SELPLG (26) or receptor X,

* Corresponding author. Mailing address: Neurovirology Project, Tokyo Metropolitan Institute of Medical Science, Tokyo Metropolitan Organization for Medical Research, 2-1-6, Kamikitazawa, Setagaya-ku, Tokyo 156-8506, Japan. Phone: 81-3-5316-3312. Fax: 81-3-5316-3224. E-mail: koike-st@igakuken.or.jp.

▽ Published ahead of print on 9 March 2011.

SCARB2 may play a central role in the early steps of EV71 infection. Therefore, characterizations of the role of SCARB2 during EV71 infection will contribute to the understanding of EV71 entry.

SCARB2 (also known as lysosomal integral membrane protein II, or CD36b like-2) belongs to the CD36 family and has two transmembrane domains, with the N and C termini located in the cytosol (10). SCARB2 is one of the most abundant proteins in the lysosomal membrane and participates in membrane transport and the reorganization of the endosomal/lysosomal compartment (21). SCARB2 also works as the receptor for the mannose-6-phosphate-independent transport of β-glucocerebrosidase (β-GC) to the lysosome (5, 30). The binding of β-GC to SCARB2 occurs within the luminal domain of SCARB2, particularly in the coiled-coil motif at amino acids 152 to 167 (30). SCARB2 deficiency in mice causes ureteropelvic junction obstruction, deafness, and peripheral neuropathy (12). Although the motifs in some cellular receptors for picornaviruses that are important for binding and/or infection have been elucidated, SCARB2 has no motifs common to other picornavirus receptors, such as an immunoglobulin (Ig)-like motif. Thus, SCARB2 is a new class of picornavirus receptor. The identification of important regions in SCARB2 would contribute to the elucidation of the virus-receptor interaction.

In this report, we compared the susceptibilities of cells expressing human SCARB2 (hSCARB2) or mouse Scarb2 (mScarb2) to EV71. Additionally, we mapped the region in hSCARB2 that is important for EV71 infection by using hSCARB2–mScarb2 chimeras.

MATERIALS AND METHODS

Cells. Human RD cells, mouse L929 cells, and African green monkey Vero cells were cultured in Dulbecco's modified Eagle medium (DMEM; Sigma) supplemented with 5% fetal bovine serum (FBS) and a penicillin-streptomycin solution (Invitrogen) (5% FBS-DMEM).

Viruses. EV71 strain SK-EV006/Malaysia/97 was propagated in Vero cells for use in this study (25). EV71-GFP, which expresses green fluorescent protein (GFP) upon viral replication, was recovered from an infectious cDNA clone, pSVA-EV71-GFP, which has been described previously (37).

Plasmids. The cDNA fragment of mScarb2 was amplified by reverse transcription-PCR (RT-PCR) from L929 cells with primers mSCARB2-Eco(+) (CAGA ATTCACCATGGGCAGATGCTGCTTCTACA) and mSCARB2-Xba(−) (CA CATCTAGATTAGGTTCGTATGAGGGGTGCT), and the PCR product was inserted into pCAGGS-PUR (14). The resulting construct was designated pCA-mScarb2. A cDNA fragment encoding mScarb2 or hSCARB2 (37) was subcloned into pCAGGS.MCS (19, 36) to create a FLAG tag at the C terminus, and the construct was designated pCA-mScarb2-F or pCA-hSCARB2-F, respectively.

Chimeric hSCARB2–mScarb2 mutants (see Fig. 6A and 7A) were constructed using standard PCR-based methods and were cloned into pCAGGS.MCS with a FLAG tag at the C terminus. The mutants did not have unexpected mutations or deletions.

Viral spread in cell culture. RD cells were infected with either EV71-GFP or EV71. At 24 h postinfection, cells infected with EV71-GFP were imaged with IX70 and DP70 cameras (Olympus) and were analyzed using DP Controller software (Olympus). The cells infected with EV71 or EV71-GFP were subsequently fixed with 4% paraformaldehyde and were probed with a mouse anti-EV71 antibody (clone 422-8D-4C-4D; Millipore), followed by incubation with an Alexa Fluor 488 donkey anti-mouse IgG (Invitrogen). Images were acquired using the IX70 camera.

PNGase F digestion. L929 cells were transfected with the plasmid encoding hSCARB2, mScarb2, hSCARB2-F, mScarb2-F, H(M4)-F, M(H2)-F, or M(H3)-F using the FuGENE 6 transfection reagent. After 48 h, the transfected cells were lysed with glycoprotein denaturing buffer (New England Biolabs [NEB]) and were then incubated for 10 min at 99°C. Denatured samples were mixed with G7 reaction buffer (NEB) supplemented with 1% NP-40 and 500 U peptide *N*-glycosidase F (PNGase F) (NEB) and were then incubated for 2 h at 37°C for digestion. These samples were mixed with a sodium dodecyl sulfate (SDS) sample buffer and were then incubated for 5 min at 95°C before being resolved on a 12% Tris-glycine gel. Resolved proteins were probed with a goat anti-hSCARB2 antibody (R&D Systems), a goat anti-mScarb2 antibody (R&D Systems), or a rabbit anti-FLAG antibody (Sigma), followed by incubation with a horseradish peroxidase (HRP)-conjugated anti-goat or anti-rabbit antibody (Jackson ImmunoResearch).

Single-round infection assay. L929 cells were transfected with the indicated plasmid in triplicate to analyze (i) transfection efficiency, (ii) protein expression, and (iii) EV71-GFP infection. Transfected cells in the first well were fixed at the plate bottom with 4% paraformaldehyde at 48 h posttransfection and were probed with the mouse anti-FLAG antibody (Sigma), followed by incubation with Alexa Fluor 488 donkey anti-mouse IgG. Images were acquired using the IX70 and DP70 cameras. Transfected cells in the second well were mixed with SDS sample buffer (Invitrogen) at 48 h posttransfection, and these samples were incubated for 5 min at 95°C before being resolved on a 12% Tris-glycine gel (Invitrogen). Resolved proteins were probed with the anti-hSCARB2 antibody, the rabbit anti-FLAG antibody (Sigma), or a mouse antibody against β-actin (ACTB) (clone AC-74; Sigma), followed by incubation with the appropriate HRP-conjugated secondary antibody (Jackson ImmunoResearch). Transfected cells in the third well were infected with EV71-GFP at 24 h after transfection and were incubated for another 24 h at 37°C. Subsequently, images were acquired using the IX70 and DP70 cameras and were analyzed using DP Controller software. Infected cells, including GFP-positive cells, were detached in trypsin-EDTA (0.05% trypsin, 0.53 mM EDTA · 4Na) (GIBCO) and were incubated with 4% paraformaldehyde for 30 min at room temperature. After being washed with phosphate-buffered saline (PBS) containing 2% FBS, the cells were analyzed with a FACSCalibur flow cytometer and CellQuest Pro software (both from Becton Dickinson and Company).

Multistep infection assay. L929 cells were transfected with the indicated plasmid using the FuGENE 6 transfection reagent. After 24 h, the transfected cells were infected with EV71 (1×10^3 50% tissue culture infective doses [$TCID_{50}$]) and were incubated for 0, 12, 24, 36, or 48 h at 37°C. At each time point, viral titers were determined and expressed as the $TCID_{50}$ according to the Reed-Muench method (31).

Immunoprecipitation assay. Pulldown assays were performed as reported previously (37) with some modifications. EV71 (1.87×10^8 $TICD_{50}$) was incubated with bovine serum albumin (BSA) (10 μg), human IgG Fc (control Fc) (10 μg; R&D Systems), hSCARB2-Fc (1, 3, or 10 μg; R&D Systems), or mScarb2-Fc (1, 3, or 10 μg; R&D Systems) and anti-human IgG (Fc specific)-agarose (Sigma) in 1 ml of 5% FBS DMEM for 2 h at 4°C. The beads were then washed twice with 5% FBS-DMEM, suspended in SDS sample buffer, and incubated for 10 min at 95°C. After the beads were removed, the samples were loaded onto a 12% Tris-glycine gel, followed by Western blotting with a rabbit anti-EV71 antibody (25) or an anti-human IgG Fc_γ fragment-specific antibody (Jackson ImmunoResearch). For deglycosylation, control Fc (3 μg) and hSCARB2-Fc (3 μg) in the native form were treated with 1,500 U PNGase F in G7 reaction buffer and were incubated for 24 h at 37°C before being mixed with anti-human IgG (Fc specific)-agarose.

Virus attachment assay. L929 cells transfected with the indicated plasmid were detached in PBS containing 0.05% EDTA. These cells were mixed with EV71 (1.87×10^8 $TICD_{50}$) for 1 h at 4°C, washed twice with 5% FBS-DMEM, suspended in SDS sample buffer, and then incubated for 10 min at 95°C. The samples were resolved by SDS-polyacrylamide gel electrophoresis (PAGE) using the 12% Tris-glycine gel, followed by Western blot analysis with an anti-EV71, anti-FLAG, or anti-ACTB antibody.

Biotinylation of cell surface proteins. L929 cells transfected with the indicated plasmids were washed twice with ice-cold PBS and were biotinylated twice with Sulfo-*N*-hydroxysuccinimide (NHS)-SS-Biotin (Pierce) for 15 min each time at 4°C. After two washes with ice-cold PBS, free thiol groups were quenched with quenching solution (Pierce), and the cells were solubilized in lysis buffer (20 mM Tris-HCl [pH 7.5], 150 mM NaCl, 1 mM EDTA, 1% Triton X-100, and Complete Mini protease inhibitor cocktail [Roche]) and were precipitated with NeutrAvidin agarose resin (Pierce). Precipitated proteins and cell lysates were analyzed by Western blotting with the anti-FLAG antibody.

RESULTS

Comparison of amino acid sequences of hSCARB2 and mScarb2. The cDNA encoding mScarb2 was prepared from

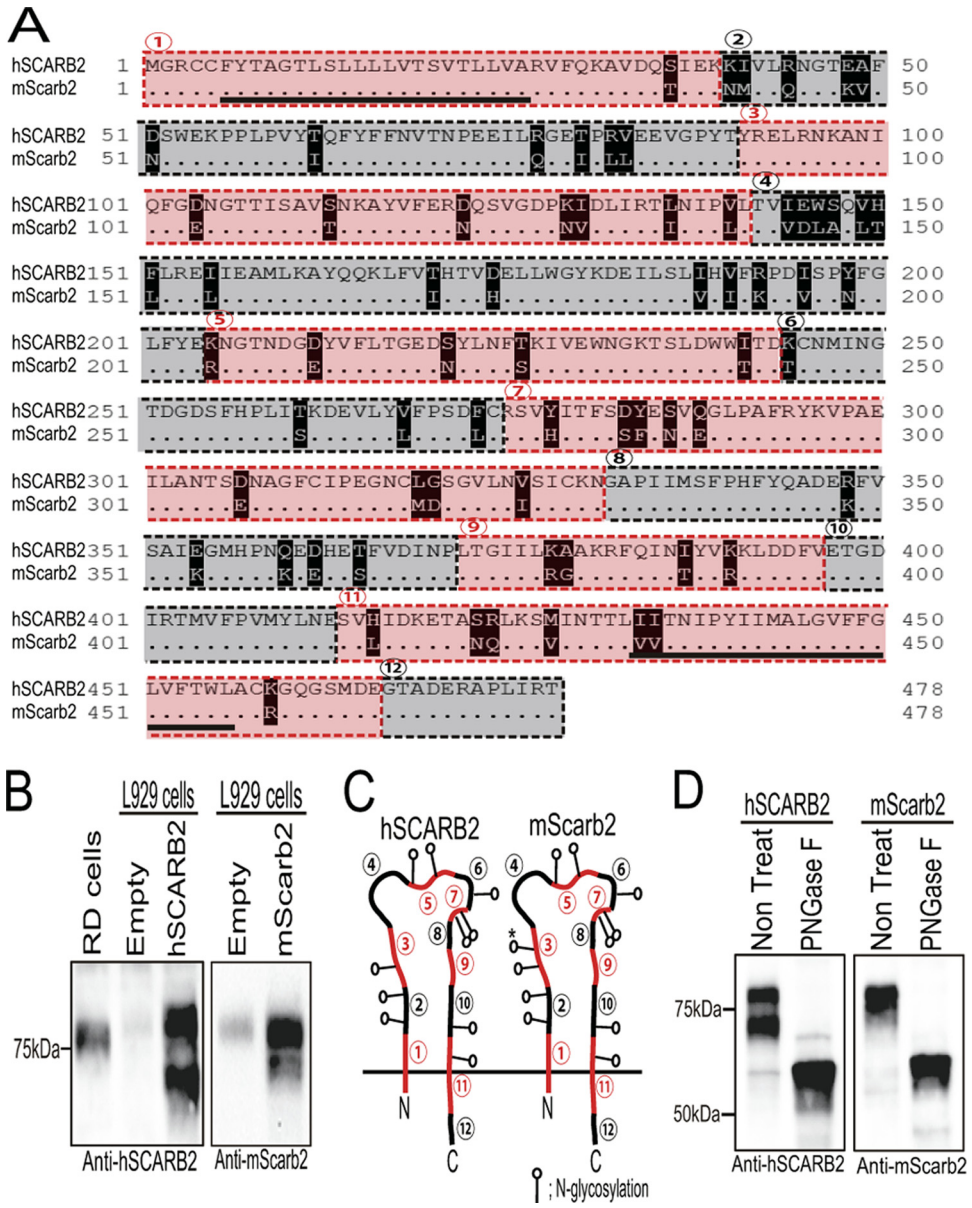

FIG. 1. Human SCARB2 and mouse Scarb2. (A) Comparison of the amino acid sequence of hSCARB2 with that of mScarb2. Divergent amino acids are highlighted. Two transmembrane domains are underlined, and the amino acids encoded in the mRNA from *SCARB2* exons 1, 3, 5, 7, 9, and 11 are outlined with red dashed lines. The amino acids encoded in the mRNA from exons 2, 4, 6, 8, 10, and 12 are outlined with black dashed lines. (B) Expression of hSCARB2 and mScarb2. L929 cells were transfected with plasmids encoding hSCARB2 or mScarb2. Transfected cells and RD cells were analyzed by Western blotting with an anti-hSCARB2 or anti-mScarb2 antibody. (C) Schematic diagrams of hSCARB2 and mScarb2. Red lines represent the amino acid sequences encoded in exons 1, 3, 5, 7, 9, and 11, and black lines represent those encoded in exons 2, 4, 6, 8, 10, and 12 (numbering from the N terminus to the C terminus). Potential N-glycosylation sites are indicated by lollipops. An asterisk marks the N-glycosylation site that is present only in mScarb2. (D) PNGase F treatment of hSCARB2 and mScarb2. L929 cells were transfected with plasmids encoding hSCARB2 or mScarb2. The cells were either left untreated (Non Treat) or treated with PNGase F, and the samples were analyzed by Western blotting with an anti-hSCARB2 or an anti-mScarb2 antibody.

L929 cells, and its amino acid sequence was compared with that of hSCARB2 (Fig. 1A). Both hSCARB2 and mScarb2 are composed of 478 amino acids, which are encoded in 12 exons. The level of amino acid identity between hSCARB2 and mScarb2 was 85.8%, and the level of similarity was 99.9%. We transiently expressed hSCARB2 and mScarb2 in L929 cells and detected the expressed proteins using anti-human and anti-mouse SCARB2 antibodies. We detected a single band that migrated at approximately 80 kDa in the Western blot of RD cells with anti-hSCARB2 antibody. mSCARB2, which is endogenously expressed in L929 cells, was detected in empty-vector-transfected L929 cells with an anti-mScarb2 antibody (Fig. 1B). We detected two major molecular species migrating at approximately 70 kDa and 80 kDa with an anti-hSCARB2 antibody in cells transfected with pCA-hSCARB2 (Fig. 1B, left). Similarly, we also detected two major molecular species

migrating at approximately 70 kDa and 80 kDa with an anti-mScarb2 antibody in cells transfected with pCA-mScarb2 (Fig. 1B, right). The apparent molecular sizes of these bands were larger than that deduced from the amino acid sequence (approximately 54 kDa). hSCARB2 and mScarb2 are reported to be N-glycosylated proteins in human and mouse cells, respectively (5, 30). hSCARB2 was found to have 10 potential N-glycosylation sites, whereas mScarb2 was found to have 11 (Fig. 1C). Potential N-glycosylation sites were found in the amino acid sequences encoded in exons 2, 3, 5, 6, 7, 10, and 11 of both hSCARB2 and mScarb2. mScarb2 had one additional potential N-glycosylation site in exon 3. To confirm whether exogenously expressed SCARB2s were glycosylated in L929 cells, cell lysates were treated with PNGase F, which removes all N-linked carbohydrate residues. After PNGase F treatment, hSCARB2 and mScarb2 were each detected as a single band at the calculated molecular mass (approximately 54 kDa) (Fig. 1D). These results indicate that hSCARB2 and mScarb2 are expressed as N-glycosylated proteins in mouse L929 cells and that the glycosylation pattern differs slightly from that of the endogenous proteins.

Strategy for the comparison of infection efficiencies in L929 cells expressing hSCARB2 or mScarb2. To compare the efficiency of a single round of EV71 infection via hSCARB2 versus mScarb2, we used EV71-GFP as a challenge virus. EV71-GFP, when used to infect cells, expresses sufficient levels of GFP to monitor the establishment of infection. This virus, however, had a defect in growth kinetics and in spreading. It was impossible to determine the viral titer either by plaque formation or by the $TCID_{50}$ method. When RD cells were infected with EV71-GFP at an appropriate dilution, GFP-positive cells became visible at approximately 16 to 18 h postinfection, suggesting that the kinetics of viral protein expression was unusual compared with that of wild-type virus. Clusters of GFP-positive or viral antigen-positive cells, which had spread from the initial infectious center, were not observed at 24 h postinfection (Fig. 2A, left and center). In contrast, when RD cells were infected with wild-type EV71, we observed clusters of viral antigen-positive cells that had formed due to spreading from the infectious centers at 24 h postinfection (Fig. 2A, right panel). Therefore, we evaluated the efficiency of EV71 infection at the initial round of infection by using EV71-GFP and counting the number of GFP-positive cells at 24 h postinfection.

To monitor the expression levels of hSCARB2 and mScarb2 by Western blotting, we added a FLAG epitope tag to the C termini of the proteins (5). To examine whether the C-terminal FLAG tag affected EV71 infection, we compared the numbers of GFP-positive cells after infection with EV71-GFP in L929 cells expressing hSCARB2 with or without the FLAG tag (Fig. 2B to E). L929 cells were transfected with pCA-hSCARB2 or pCA-hSCARB2-F, and after 24 h, the transfection efficiencies and expression of hSCARB2 and hSCARB2-F were confirmed by immune staining and Western blot analysis, respectively (Fig. 2B and C). The numbers of SCARB2-positive cells in L929 cells transfected with pCA-hSCARB2 or pCA-hSCARB2-F were comparable (Fig. 2B). Two major species of hSCARB2 and hSCARB2-F with similar intensities were detected by Western blotting using the anti-hSCARB2 antibody (Fig. 2C). Thus, the transfection efficiency, expression level, and glycosylation pattern of hSCARB2 were not affected by the addition of the FLAG tag. Under these conditions, these transfected L929 cells were infected with EV71-GFP and were imaged at 24 h postinfection (Fig. 2D). No GFP-positive cells were observed in the mock-transfected or empty-plasmid-transfected cells, whereas many GFP-positive cells were detected in the hSCARB2- and hSCARB2-F-transfected cells (Fig. 2D). To quantify the microscopic observations, these cells were analyzed by fluorescence-activated cell sorting (FACS) to

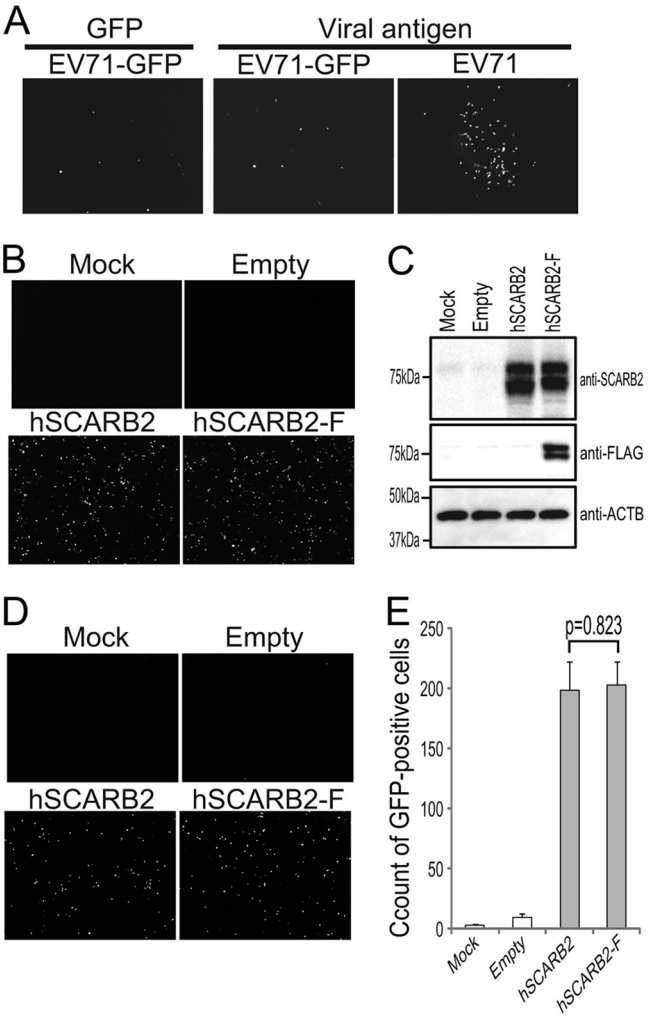

FIG. 2. Strategy for comparing infection efficiencies in L929 cells expressing hSCARB2 or mScarb2. (A) EV71-GFP is defective in viral spread. RD cells were infected with EV71 or EV71-GFP. Infected cells were imaged at 24 h postinfection in order to observe GFP via fluorescence microscopy (GFP) and were then stained with an anti-EV71 antibody. (B to E) Efficiency of EV71-GFP infection via hSCARB2 with or without the FLAG tag. (B) Transfection efficiency was assessed by immunostaining with an anti-hSCARB2 antibody. (C) Expression of hSCARB2 or hSCARB2-F was confirmed by Western blot analysis with an anti-hSCARB2 or an anti-FLAG antibody. Expression of β-actin (ACTB) was used as a loading control. (D and E) Cells infected with EV71-GFP were imaged via fluorescence microscopy (D) and were concomitantly analyzed by FACS to quantify the number of GFP-positive cells (E). The FACS data are shown as mean counts with standard deviations ($n = 3$). Statistical significance was determined by Student's t test. There was no significant difference between hSCARB2 and hSCARB2-F ($P = 0.823$).

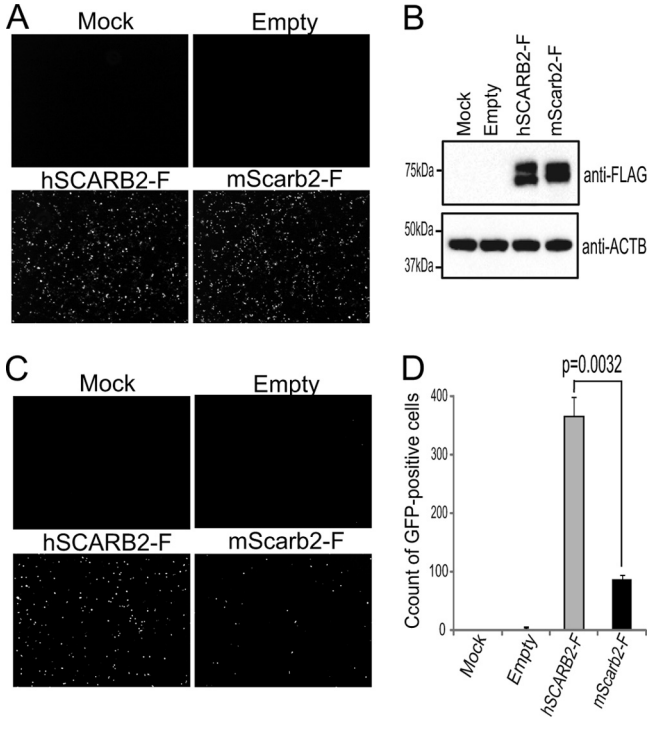

FIG. 3. Efficiencies of EV71-GFP infection via hSCARB2 or mScarb2. Single-round infection assays were performed to compare the efficiencies of EV71 infection via hSCARB2-F versus mScarb2-F. (A and B) The transfection efficiencies and expression of hSCARB2-F and mScarb2-F were confirmed by immunostaining (A) and Western blot analysis with an anti-FLAG antibody (B), respectively. ACTB was used as a loading control for the Western blot. (C and D) The transfected cells infected with EV71-GFP were imaged via fluorescence microscopy (C) and were then analyzed by FACS (D). The FACS data are shown as mean counts with standard deviations ($n = 3$). Statistical significance was determined by Student's t test.

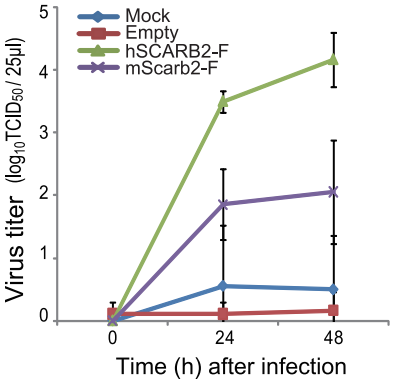

FIG. 4. Multistep infections of EV71 in L929 cells expressing hSCARB2 or mScarb2. Mock-transfected L929 cells and cells transfected with an empty plasmid or with a plasmid encoding hSCARB2-F or mScarb2-F were infected with EV71 at a low MOI. Viral titers in Vero cells were determined at 0, 24, and 48 h postinfection. The data are shown as mean viral titers with standard deviations ($n = 3$).

count the number of GFP-positive cells (Fig. 2E). As reported previously, the number of GFP-positive cells was significantly greater in cells expressing hSCARB2 or hSCARB2-F than in mock- or empty plasmid-transfected cells ($P < 0.01$) (37). There was no significant difference in the number of GFP-positive cells between hSCARB2- and hSCARB2-F-expressing cells ($P = 0.823$). Similar results were obtained using nontagged and FLAG-tagged mScarb2 (data not shown). These results clearly show that EV71 infection via SCARB2 was not affected by the C-terminal FLAG tag. From these results, we could compare the efficiencies of EV71-GFP infection using this assay.

EV71-GFP infection of L929 cells expressing hSCARB2 and mScarb2. We conducted the single-round infection assay to compare the efficiencies of EV71 infection in L929 cells expressing hSCARB2-F versus mScarb2-F (Fig. 3). L929 cells were either mock transfected or transfected with pCA-hSCARB2-F, pCA-mScarb2-F, or an empty plasmid. After confirmation of transfection efficiency and expression of hSCARB2-F and mScarb2-F by immune staining and Western blotting (Fig. 3A and B), the transfected cells were infected with EV71-GFP and were observed at 24 h postinfection (Fig. 3C). No GFP-positive cells were found in mock- or empty-plasmid-transfected cells. A large number of GFP-positive cells were detected in hSCARB2-F-transfected cells, whereas a modest number were detected in mScarb2-F-transfected cells (Fig. 3C). By FACS analysis, the number of GFP-positive cells was significantly greater in L929 cells expressing hSCARB2-F than in those expressing mScarb2-F ($P = 0.0032$) (Fig. 3D). These results indicate that EV71-GFP infected efficiently via hSCARB2 and less efficiently via mScarb2 and that the efficiencies of infection by use of the two receptors were significantly different.

Multistep EV71 infection of L929 cells expressing hSCARB2 and mScarb2. To validate the results obtained with the single-round infection experiment using EV71-GFP, we performed a multistep infection assay with wild-type EV71 infecting at a low multiplicity of infection (MOI) to examine the spread of the virus. We confirmed by immune staining and Western blotting that hSCARB2-F and mScarb2-F were transfected and expressed at similar levels (data not shown). L929 cells expressing hSCARB2-F and mScarb2-F were infected with EV71, and the viral titers were determined at each time point (Fig. 4). EV71 grew efficiently in L929 cells expressing hSCARB2-F but only moderately in L929 cells expressing mScarb2-F. At the last time point, the viral titer in L929 cells expressing hSCARB2-F was approximately 100-fold higher than that in L929 cells expressing mScarb2-F. EV71 propagated minimally in mock-transfected and empty-plasmid-transfected L929 cells. These results indicate that EV71 infected more efficiently via hSCARB2 than via mScarb2.

Binding of hSCARB2 and mScarb2 to EV71. To elucidate the functional difference between hSCARB2 and mScarb2 in the early steps of infection, we conducted pulldown assays to compare the binding affinities of soluble hSCARB2-Fc and soluble mScarb2-Fc for EV71 (Fig. 5A). EV71 was incubated with BSA, control Fc, hSCARB2-Fc, or mScarb2-Fc and with anti-Fc-agarose beads, and precipitated proteins were analyzed by Western blotting. EV71 VP1 was detected at all concentrations of hSCARB2-Fc, and the amount of precipitated VP1 increased in a concentration-dependent manner, as reported previously (37). However, while mScarb2-Fc was precipitated at a level similar to that of hSCARB2-Fc at each concentration

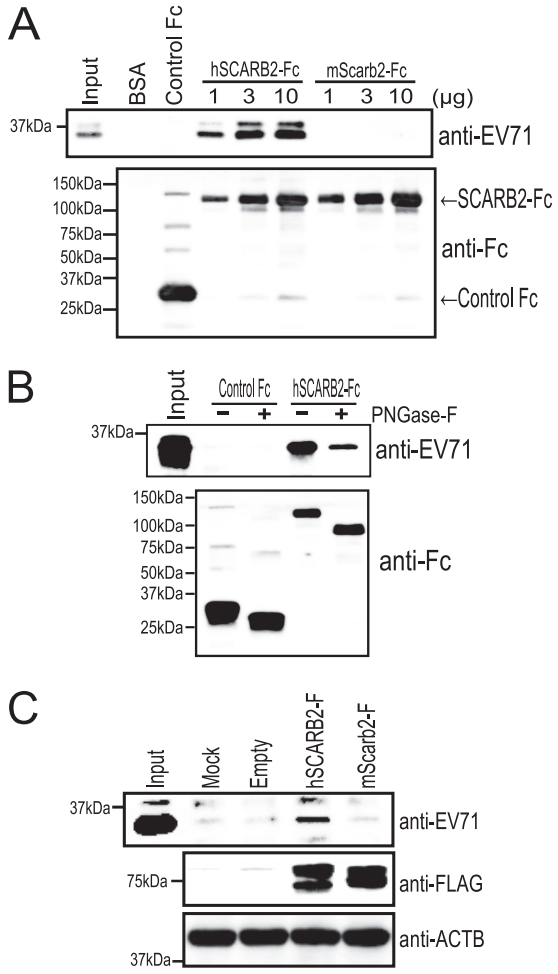

FIG. 5. Binding of hSCARB2 to EV71. (A) hSCARB2-Fc bound to EV71. A total of 10 μg of BSA, 10 μg of control Fc, or 1, 3, or 10 μg of hSCARB2-Fc or mScarb2-Fc was bound to anti-human Fc-agarose and was incubated with EV71. The precipitated proteins were analyzed by Western blotting with an anti-EV71 or anti-Fc antibody. The anti-EV71 antibody detected primarily the viral VP1 protein. (B) hSCARB2-Fc with or without N-linked carbohydrate chains bound to EV71. EV71 was incubated with 3 μg of control Fc or 3 μg of hSCARB2-Fc treated with PNGase F, and the proteins were precipitated with an anti-Fc antibody. The precipitated proteins were analyzed by Western blotting with an anti-EV71 or anti-Fc antibody. (C) EV71 attached to hSCARB2-expressing L929 cells. L929 cells were either mock transfected or transfected with an empty plasmid, pCA-hSCARB2-F, or pCA-mScarb2-F. The transfected cells were incubated with EV71 at 4°C. After the wash steps, the cells were lysed and analyzed by Western blotting with an anti-EV71, anti-FLAG, or anti-ACTB antibody. ACTB was used as a loading control.

(Fig. 5A, lower panel), VP1 was not detected at any concentration of mScarb2-Fc (Fig. 5A, upper panel). VP1 did not precipitate with BSA or control Fc. These data show that the binding affinity of hSCARB2 for EV71 was stronger than that of mScarb2.

To determine whether the N-linked carbohydrate chains of hSCARB2 contribute to the binding to virions, the native form of hSCARB2-Fc was treated with PNGase F. The removal of the carbohydrate chains from hSCARB2-Fc was confirmed by the 25-kDa downward size shift observed by Western blotting in the protein treated with PNGase F. PNGase F-treated hSCARB2-Fc or untreated hSCARB2-Fc was mixed with virions. After immunoprecipitation, bound virions and Fc proteins were analyzed by Western blotting (Fig. 5B). EV71 coprecipitated with both PNGase F-treated and nontreated hSCABR2-Fc; however, the intensity of the EV71 VP1 band coprecipitating with PNGase F-treated hSCARB2-Fc was only moderately lower than that of the band coprecipitating with nontreated hSCARB2-Fc. These results indicate that the carbohydrate chains of hSCARB2 are not essential for the EV71–hSCARB2 interaction.

To assess the binding of EV71 to SCARB2 at the plasma membrane, we performed virus attachment assays using a transient expression system (Fig. 5C). L929 cells were either mock transfected or transfected with an empty plasmid, pCA-hSCARB2-F, or pCA-mScarb2-F. The expression level of hSCARB2-F was similar to that of mScarb2-F (Fig. 5C, center). After 48 h posttransfection, these cells were mixed with EV71, washed to remove unbound virus, lysed together with bound viruses, and then analyzed by Western blotting. The amount of EV71 that was bound to cells transfected with pCA-hSCARB2 was substantially greater than that bound to mock-transfected cells or to cells transfected with an empty plasmid or pCA-mScarb2 (Fig. 5C, top). These data show that the binding affinity of EV71 for hSCARB2 in the membrane was stronger than that for mScarb2 in the membrane.

Determination of the hSCARB2 region that mediates EV71 infection. Because EV71 infected L929 cells more efficiently via hSCARB2 than via mScarb2 (Fig. 4), we mapped the region(s) that was important for EV71 infection by using chimeric hSCARB2–mScarb2 mutants. We hypothesized that the efficiency of EV71 infection via hSCARB2 would be lowered by replacement of the important region(s) with the corresponding region(s) in mScarb2 and vice versa. For this purpose, we prepared 6 chimeric mutants in which some of the exons were replaced (Fig. 6A). In the H(M1-4)-F mutant, for example, the human amino acid sequence 1 to 204, encoded in *hSCARB2* exons 1 to 4, was replaced with the corresponding region from mScarb2. Other chimeric mutants were constructed according to the same strategy. We performed the single-round infection assay to compare the efficiencies of EV71-GFP infection via these chimeras. All mutants were transfected and expressed at similar levels (Fig. 6B). Transfected cells were infected with EV71-GFP and were imaged with a microscope at 24 h postinfection (data not shown). These cells were analyzed by FACS to count the number of GFP-positive cells (Fig. 6C). Among the hSCARB2 backbone chimeric mutants, the H(M1-4)-F mutant failed to mediate efficient EV71-GFP infection. Among the mScarb2 backbone chimeras, the M(H1-4)-F mutant mediated efficient EV71-GFP infection. These data indicate that the region from amino acids 1 to 204, encoded in human *SCARB2* exons 1 to 4, is important for EV71-GFP infection.

To refine the region important for EV71-GFP infection, we constructed an additional 8 chimeric mutants in each of which one of exons 1 to 4 was replaced (Fig. 7A). The transfection efficiencies of all chimeric mutants were comparable (data not shown). Expression of chimeric mutants in L929 cells was confirmed by Western blotting (Fig. 7B). We found that the levels of expression of mutants H(M1)-F, H(M2)-F, H(M3)-F,

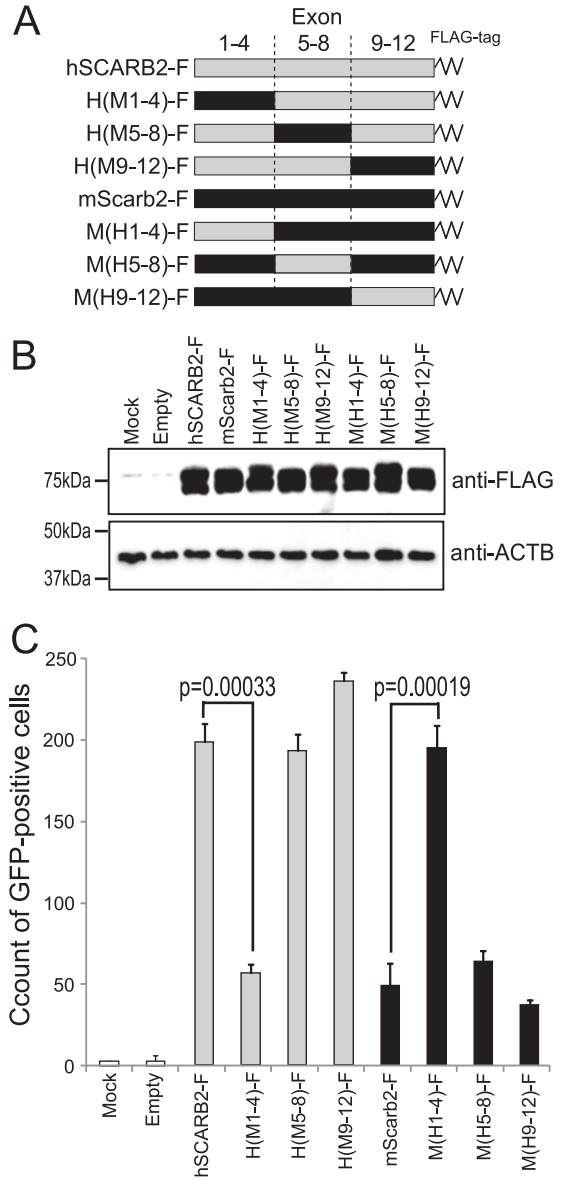

FIG. 6. Amino acids 1 to 204 of hSCARB2 are important for efficient EV71 infection. (A) Schematic diagram of chimeric hSCARB2–mScarb2 mutants. A series of mutants was constructed by the sequential substitution of a set of 4 exons. A FLAG tag was added at the C terminus of the open reading frame. (B and C) Single-round infection assays were performed to compare the efficiencies of EV71 infection as described in the legend to Fig. 3. FACS data are shown as mean counts with standard deviations ($n = 3$). Statistical significance was determined by Student's t test.

M(H1)-F, and M(H4)-F were comparable to that of hSCARB2-F, and the ratios of the two major molecular species migrating at approximately 80 kDa and 70 kDa were similar to that for hSCARB2-F. Two species of approximately 80 kDa and 70 kDa for H(M4)-F and M(H3)-F were detected; however, the intensity of the 80-kDa species in H(M4)-F and M(H3)-F was lower than that in hSCARB2. In M(H2)-F-transfected cells, we detected at least 3 species migrating at approximately 55 kDa, 80 kDa, and 90 kDa. Treatment of wild-type SCARB2-F and the three chimeric mutants with PNGase F resulted in similar apparent molecular masses (Fig. 7D). This result shows that the differences in the mobility and the ratios of these species between these three mutants were caused by differing N-glycosylation patterns and not by protein degradation. Replacement of a region in hSCARB2 with the corresponding region in mScarb2, and vice versa, may affect protein folding and it may contribute to the difference in N-glycosylation patterns. We performed the single-round infection assay to determine the infection efficiency. The transfected cells were infected with EV71-GFP and were analyzed by FACS to count the number of GFP-positive cells (Fig. 7C). In a series of experiments using the hSCARB2 backbone chimeras, the number of GFP-positive cells in cells expressing H(M4)-F was significantly decreased ($P = 0.000039$). In experiments using the mScarb2 backbone chimeras, the number of GFP-positive cells in cells expressing M(H4)-F was significantly greater ($P = 0.00071$). These data indicate that the region from amino acids 142 to 204, encoded in *SCARB2* exon 4, is important for EV71-GFP infection.

To further refine the region important for EV71 infection, we constructed 4 chimeric mutants in which the first or second half of exon 4 was replaced with the sequence of the other species of origin, and we analyzed infection efficiency with the single-round infection assay. Each mutant showed an infection efficiency intermediate between those of hSCARB2 and mScarb2 (data not shown). These data indicate that the important amino acids for EV71 infection are localized throughout the region from amino acids 142 to 204.

Multistep infection of L929 cells expressing H(M4)-F or M(H4)-F. In order to confirm the important region identified by the single-round infection assay, we carried out multistep infection assays to determine the spread of wild-type EV71 in chimera-expressing L929 cells. L929 cells were transfected with plasmids encoding hSCARB2-F, mScarb2-F, H(M4)-F, or M(H4)-F and were subsequently infected with EV71. Viral titers were determined at each time point (Fig. 8). EV71 grew as efficiently in L929 cells expressing M(H4)-F as in L929 cells expressing hSCARB2-F, whereas EV71 grew at a moderate level in L929 cells expressing M(H4)-F or mScarb2-F. The final viral titer in L929 cells expressing hSCARB2-F or M(H4)-F was approximately 40-fold higher than that in L929 cells expressing mScarb2-F or H(M4)-F. These results indicate that the M(H4)-F mutant functioned as a receptor for EV71 with an efficiency similar to that of hSCARB2-F.

Binding of H(M4)-F and M(H4)-F to EV71. Because the region from amino acids 142 to 204 was important for the single and multistep EV71 infections, we presumed that this region played a critical role in the binding of EV71. Before a virus attachment assay was performed, the expression of hSCARB2-F, mScarb2-F, H(M4)-F, and M(H4)-F on the cell surface was confirmed by biotinylation of cell surface proteins (Fig. 9A). Similar amounts of biotinylated hSCARB2-F, mScarb2-F, H(M4)-F, and M(H4)-F were precipitated with NeutrAvidin agarose resin. Without biotinylation, no FLAG-tagged receptors were precipitated. These results indicate that these receptors were expressed comparably at the cell surface. Next, L929 cells transfected with a plasmid encoding hSCARB2-F, mScarb2-F, H(M4)-F, or M(H4)-F were mixed with EV71, and bound viruses were detected by Western blotting. The amount of EV71 VP1 that bound to cells expressing

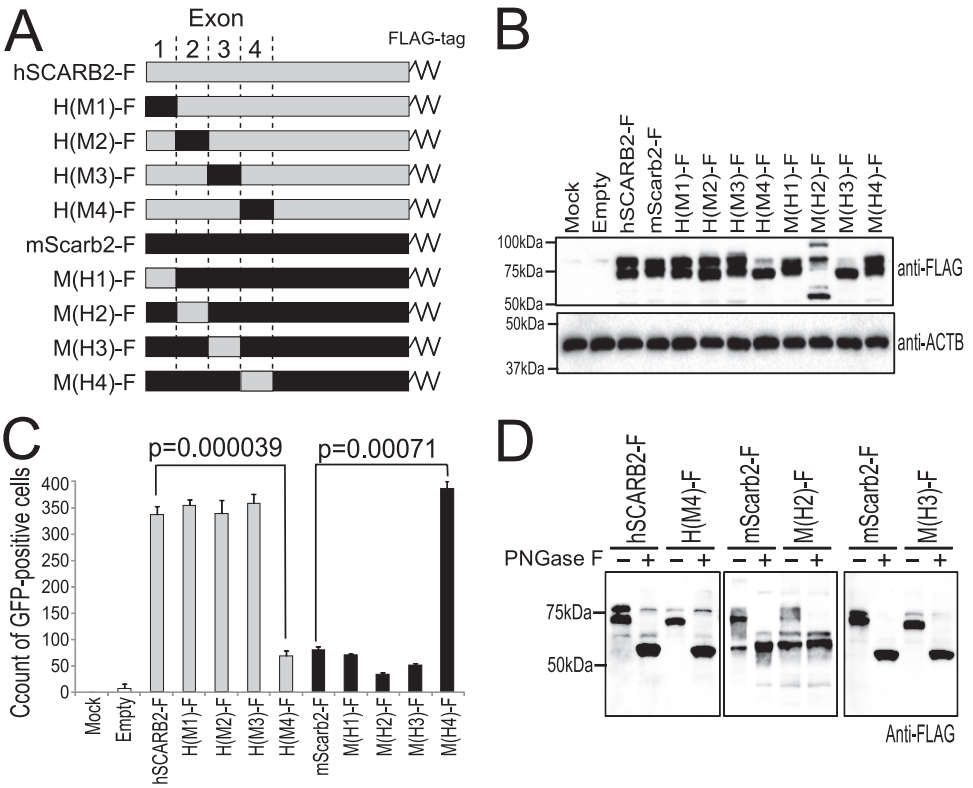

FIG. 7. The region from amino acids 142 to 204 of hSCARB2 is important for efficient EV71 infection. (A) Schematic diagram of chimeric hSCARB2–mScarb2 mutants. A series of mutants was constructed by the substitution of exons 1 to 4 individually. A FLAG tag was added at the C terminus of the open reading frame. (B and C) Single-round infection assays. (B) Expression of hSCARB2-F, mScarb2-F, and chimeric receptors was confirmed by Western blot analysis with an anti-FLAG antibody. ACTB was used as a loading control for the Western blot. (C) Transfected cells infected with EV71-GFP were analyzed by FACS. The FACS data are shown as mean counts with standard deviations ($n = 3$). Statistical significance was determined by Student's t test. (D) PNGase F treatment of H(M4)-F, M(H2)-F, and M(H3)-F. L929 cells were transfected with a plasmid encoding H(M4)-F, M(H2)-F, or M(H3)-F. The cells were treated with PNGase F, and the samples were analyzed by Western blotting with an anti-FLAG antibody.

hSCARB2-F or M(H4)-F was clearly larger than that for cells that were either mock transfected or transfected with an empty plasmid, mScarb2-F, or H(M4)-F. These results indicate that M(H4)-F bound to EV71 at a level similar to that of hSCARB2-F.

DISCUSSION

The viral receptor plays multiple roles, including the key steps for viral entry, viral attachment, possible internalization, and/or uncoating. We have shown that EV71 efficiently infected mouse cells via hSCARB2 but not via mScarb2. Using soluble receptors and receptor-expressing cells, we demonstrated that hSCARB2, but not mScarb2, bound efficiently to EV71. The binding of mScarb2 to EV71 was too weak to detect under our experimental conditions. We conclude that the ability of SCARB2 molecules to bind to EV71 virions is at least one of the major functional differences between hSCARB2 and mScarb2. Other receptor roles, such as internalization and uncoating, in the SCARB2 molecule require elucidation in further studies.

We have mapped the region of human SCARB2 that is important for both efficient virus binding and the establishment of infection to amino acids 142 to 204 by using human SCARB2 and mouse Scarb2 chimeric receptors. The overall amino acid identity between hSCARB2 and mScarb2 was 85.8%, while the local amino acid identity of amino acids 142 to 204 was 76.2%. EV71 binds a region that is divergent for the human and mouse sequences. Amino acids 142 to 204 may form the core region of the binding site for virions. We prepared a fusion protein consisting of amino acids 142 to 204 of hSCARB2 and the Fc region of human IgG (H4-Fc) in order to determine whether this region was sufficient for virus binding. However, an attempt to precipitate EV71 with H4-Fc was not successful (data not shown). This failure suggested two possibilities: either that that H4 region, which would have been sufficient for virus binding, was not folded appropriately in the fusion protein or that some amino acids outside this region, which are common to the human and mouse sequences, participate in the interaction. Recently, it was reported that a coiled-coil domain of SCARB2/LIMPII at positions 152 to 167, which included the region important for EV71 infection and binding, is necessary for β-GC binding (5). This report indicates that the region from amino acids 142 to 204 is potentially exposed on the surface of the protein.

There is no potential N-glycosylation site in the region from amino acids 142 to 204 of hSCARB2 or mScarb2. Moreover, we showed that the N-linked carbohydrate chains of hSCARB2

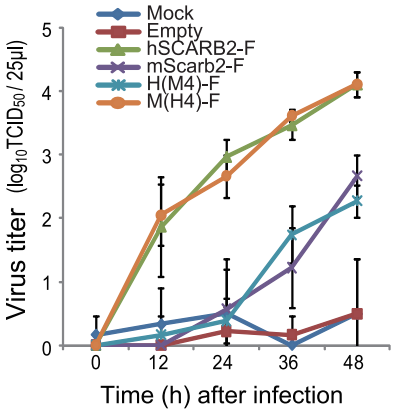

FIG. 8. Multistep infections of EV71. Mock-transfected L929 cells and cells transfected with an empty plasmid or a plasmid encoding hSCARB2-F, mScarb2-F, H(M4)-F, or M(H4)-F were infected with EV71 at a low MOI. Viral titers in Vero cells were determined at 0, 12, 24, 36, and 48 h postinfection. The data are shown as mean viral titers with standard deviations ($n = 3$).

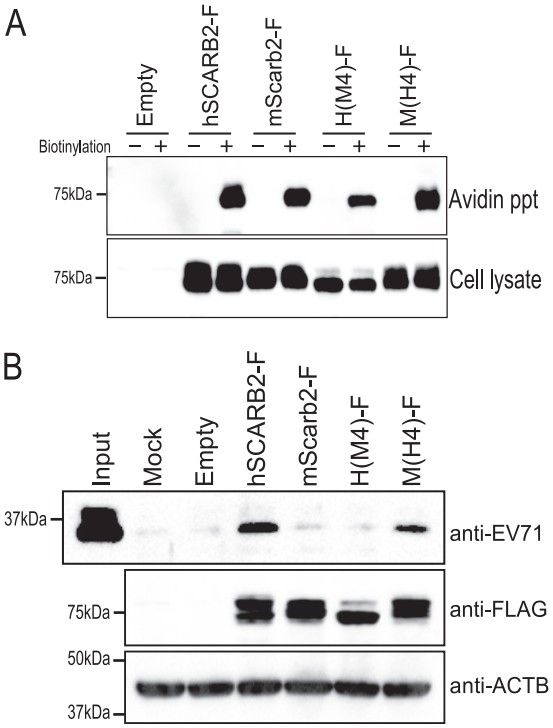

FIG. 9. The M(H4)-F mutant bound to EV71 as efficiently as hSCARB2-F. (A) Biotinylation of cell surface proteins. L929 cells were transfected with an empty plasmid, pCA-hSCARB2-F, pCA-mScarb2-F, pCA-H(M4)-F, or pCA-M(H4)-F. Cell surface proteins of transfected cells were biotinylated and precipitated with NeutrAvidin agarose resin. Precipitated proteins (Avidin ppt) and total-cell lysates (Cell lysate) were analyzed by Western blotting with the anti-FLAG antibody. (B) Binding of EV71 to chimeras. L929 cells were either mock transfected or transfected with an empty plasmid, pCA-hSCARB2-F, pCA-mScarb2-F, pCA-H(M4)-F, or pCA-M(H4)-F. These cells were incubated with EV71 at 4°C. After the wash steps, the cells and bound viruses were lysed and analyzed by Western blotting with an anti-EV71 or anti-FLAG antibody. ACTB was used as a loading control.

were not essential for the EV71–hSCARB2 interaction. Taken together, the results suggest that direct protein-protein interaction is essential for the EV71–SCARB2 interaction. However, in immunoprecipitation experiments using soluble hSCARB2-Fc, hSCARB2-Fc treated with PNGase F coprecipitated reduced amounts of EV71. Therefore, we cannot exclude the possibility that N-linked carbohydrate chains play some role in the binding of hSCARB2 to EV71, such as bridging of the EV71–hSCARB2 interaction or stabilization of the conformation of hSCARB2.

Several types of picornavirus receptors have been identified and characterized. Each type of receptor has characteristics common to the family. Receptors of the first type, which include poliovirus receptor (PVR), intercellular adhesion molecule 1 (ICAM-1) of major group rhinoviruses, human coxsackievirus B and adenovirus 2 receptor (HCAR) of coxsackievirus B1 to B6, and vascular cell adhesion molecule 1 (VCAM-1) of encephalomyocarditis virus (EMCV), are members of the immunoglobulin superfamily whose extracellular regions have two to seven Ig-like domains (9, 15, 18, 20). These type II transmembrane receptors sterically bind to the virus canyon at the distal Ig-like domain (D1) through multiple amino acids (22, 34). Receptors of the second type, the $\alpha_v\beta_1$, $\alpha_v\beta_3$, and $\alpha_v\beta_6$ integrins of parechovirus, cocsackievirus A9, and foot-and-mouth disease virus (FMDV), belong to the integrin family and bind to an exposed RGD motif on the virion surface via their α or β chain (7, 34, 35, 38). Receptors of the third type, which include low-density lipoprotein receptor (LDL-R) of minor group rhinoviruses and decay-accelerating factor (DAF) of some echoviruses and group B coxsackieviruses, bind outside the canyon via complement type A repeats and short consensus repeats (SCRs), respectively (4, 9, 16). Although SCARB2 does not belong to the immunoglobulin superfamily or the integrin family, we identified the region (amino acids 142 to 204) of hSCARB2 that mediates viral attachment and infection. In this region, multiple amino acids spanning the entire region from 142 to 204 are important for binding and infection. Similar results have been shown for the D1 region of PVR. Three main sites have been found to be important for poliovirus binding: (i) the C-C′ loop through the C″ strand, (ii) the border of the D strand and the D-E loop, and (iii) the G strand (2, 3, 15, 24, 29). Therefore, hSCARB2 binds to EV71 with multiple contact points, which suggests that the region spanning amino acids 142 to 204 of hSCARB2 may bind to the viral canyon in a manner similar to the interaction between poliovirus and PVR. The crystallization of the EV71 virions and SCARB2 or the cocrystallization of EV71 with SCARB2 should reveal the EV71–SCARB2 interaction at the atomic level. The identification of the region in hSCARB2 that mediates binding and infection would bring new insight into the nature of the virus-receptor interaction of picornaviruses, and further studies would contribute to a thorough understanding of the binding of EV71 to the receptor.

In summary, our data have shown that amino acids 142 to 204 (encoded in human *SCARB2* exon 4) of SCARB2 are important for EV71 infection and binding. The identification of this region of human SCARB2 that is required for the EV71 infection greatly contributes to the understanding of virus-receptor interactions, because human SCARB2 has no known

picornavirus receptor motifs. Further studies would clarify the early steps of EV71 infection. The replacement of exon 4 of mouse *Scarb2* with the corresponding human SCARB2 sequence will lead to the development of a new mouse model susceptible to EV71. These mice will greatly contribute to the understanding of EV71 neuropathogenicity *in vivo* and possibly to the development of a vaccine and/or an antiviral drug.

ACKNOWLEDGMENTS

We thank H. Shimizu and Y. Nishimura (NIDD of Japan) for providing us with EV71 strain SK-EV006/Malaysia/97 and for helpful discussions, Y. Kawaoka (University of Tokyo) for providing us with pCAGGS.MCS, and K. Fujii for useful discussions and critical reading of the manuscript.

This work was supported in part by a Grant-in-Aid for Scientific Research (C) (20590243) from the Japan Society for the Promotion of Science, in part by a Grant-in-Aid for Young Scientists (B) (21790454) from the Ministry of Education, Culture, Sports, Science and Technology (MEXT), and in part by a Grant-in-Aid for Research on Emerging and Re-emerging Infectious Diseases from the Ministry of Health, Labor and Welfare of Japan.

REFERENCES

1. **Ahmad, K.** 2000. Hand, foot, and mouth disease outbreak reported in Singapore. Lancet **356:**1338.
2. **Aoki, J., S. Koike, I. Ise, Y. Sato-Yoshida, and A. Nomoto.** 1994. Amino acid residues on human poliovirus receptor involved in interaction with poliovirus. J. Biol. Chem. **269:**8431–8438.
3. **Belnap, D. M., et al.** 2000. Three-dimensional structure of poliovirus receptor bound to poliovirus. Proc. Natl. Acad. Sci. U. S. A. **97:**73–78.
4. **Bergelson, J. M., et al.** 1994. Decay-accelerating factor (CD55), a glycosylphosphatidylinositol-anchored complement regulatory protein, is a receptor for several echoviruses. Proc. Natl. Acad. Sci. U. S. A. **91:**6245–6248.
5. **Blanz, J., et al.** 2010. Disease-causing mutations within the lysosomal integral membrane protein type 2 (LIMP-2) reveal the nature of binding to its ligand beta-glucocerebrosidase. Hum. Mol. Genet. **19:**563–572.
6. **Blomberg, J., et al.** 1974. New enterovirus type associated with epidemic of aseptic meningitis and-or hand, foot, and mouth disease. Lancet **ii:**112. (Letter.)
7. **Burman, A., et al.** 2006. Specificity of the VP1 GH loop of foot-and-mouth disease virus for αv integrins. J. Virol. **80:**9798–9810.
8. **Chan, L. G., et al.** 2000. Deaths of children during an outbreak of hand, foot, and mouth disease in Sarawak, Malaysia: clinical and pathological characteristics of the disease. For the Outbreak Study Group. Clin. Infect. Dis. **31:**678–683.
9. **Coyne, C. B., and J. M. Bergelson.** 2006. Virus-induced Abl and Fyn kinase signals permit coxsackievirus entry through epithelial tight junctions. Cell **124:**119–131.
10. **Eskelinen, E. L., Y. Tanaka, and P. Saftig.** 2003. At the acidic edge: emerging functions for lysosomal membrane proteins. Trends Cell Biol. **13:**137–145.
11. **Fujimoto, T., et al.** 2002. Outbreak of central nervous system disease associated with hand, foot, and mouth disease in Japan during the summer of 2000: detection and molecular epidemiology of enterovirus 71. Microbiol. Immunol. **46:**621–627.
12. **Gamp, A. C., et al.** 2003. LIMP-2/LGP85 deficiency causes ureteric pelvic junction obstruction, deafness and peripheral neuropathy in mice. Hum. Mol. Genet. **12:**631–646.
13. **Hagiwara, A., I. Tagaya, and T. Yoneyama.** 1978. Epidemic of hand, foot and mouth disease associated with enterovirus 71 infection. Intervirology **9:**60–63.
14. **Hatakeyama, S., et al.** 2005. Enhanced expression of an α2,6-linked sialic acid on MDCK cells improves isolation of human influenza viruses and evaluation of their sensitivity to a neuraminidase inhibitor. J. Clin. Microbiol. **43:**4139–4146.
15. **He, Y., et al.** 2000. Interaction of the poliovirus receptor with poliovirus. Proc. Natl. Acad. Sci. U. S. A. **97:**79–84.
16. **Hewat, E. A., et al.** 2000. The cellular receptor to human rhinovirus 2 binds around the 5-fold axis and not in the canyon: a structural view. EMBO J. **19:**6317–6325.
17. **Ho, M., et al.** 1999. An epidemic of enterovirus 71 infection in Taiwan. Taiwan Enterovirus Epidemic Working Group. N. Engl. J. Med. **341:**929–935.
18. **Huber, S. A.** 1994. VCAM-1 is a receptor for encephalomyocarditis virus on murine vascular endothelial cells. J. Virol. **68:**3453–3458.
19. **Kobasa, D., M. E. Rodgers, K. Wells, and Y. Kawaoka.** 1997. Neuraminidase hemadsorption activity, conserved in avian influenza A viruses, does not influence viral replication in ducks. J. Virol. **71:**6706–6713.
20. **Kolatkar, P. R., et al.** 1999. Structural studies of two rhinovirus serotypes complexed with fragments of their cellular receptor. EMBO J. **18:**6249–6259.
21. **Kuronita, T., et al.** 2002. A role for the lysosomal membrane protein LGP85 in the biogenesis and maintenance of endosomal and lysosomal morphology. J. Cell Sci. **115:**4117–4131.
22. **Lin, J. Y., et al.** 2009. Viral and host proteins involved in picornavirus life cycle. J. Biomed. Sci. **16:**103.
23. **McMinn, P. C.** 2002. An overview of the evolution of enterovirus 71 and its clinical and public health significance. FEMS Microbiol. Rev. **26:**91–107.
24. **Morrison, M. E., Y. J. He, M. W. Wien, J. M. Hogle, and V. R. Racaniello.** 1994. Homolog-scanning mutagenesis reveals poliovirus receptor residues important for virus binding and replication. J. Virol. **68:**2578–2588.
25. **Nagata, N., et al.** 2002. Pyramidal and extrapyramidal involvement in experimental infection of cynomolgus monkeys with enterovirus 71. J. Med. Virol. **67:**207–216.
26. **Nishimura, Y., et al.** 2009. Human P-selectin glycoprotein ligand-1 is a functional receptor for enterovirus 71. Nat. Med. **15:**794–797.
27. **Qiu, J.** 2008. Enterovirus 71 infection: a new threat to global public health? Lancet Neurol. **7:**868–869.
28. **Racaniello, V.** 2007. Picornaviridae: the viruses and their replication, p. 795–838. *In* D. M. Knipe, P. M. Howley, D. E. Griffin, R. A. Lamb, M. A. Martin, B. Roizman, and S. E. Straus (ed.), Fields virology, 5th ed. Lippincott Williams & Wilkins, Philadelphia, PA.
29. **Racaniello, V. R.** 1996. Early events in poliovirus infection: virus-receptor interactions. Proc. Natl. Acad. Sci. U. S. A. **93:**11378–11381.
30. **Reczek, D., et al.** 2007. LIMP-2 is a receptor for lysosomal mannose-6-phosphate-independent targeting of beta-glucocerebrosidase. Cell **131:**770–783.
31. **Reed, L. J., and H. Muench.** 1938. A simple method of estimating 50 percent endpoints. Am. J. Hyg. (Lond.) **27:**493–497.
32. **Rossmann, M. G., and J. E. Johnson.** 1989. Icosahedral RNA virus structure. Annu. Rev. Biochem. **58:**533–573.
33. **Schmidt, N. J., E. H. Lennette, and H. H. Ho.** 1974. An apparently new enterovirus isolated from patients with disease of the central nervous system. J. Infect. Dis. **129:**304–309.
34. **Semler, B., and E. Wimmer.** 2002. Molecular biology of picornaviruses. ASM Press, Washington, DC.
35. **Williams, C. H., et al.** 2004. Integrin $\alpha_v\beta_6$ is an RGD-dependent receptor for coxsackievirus A9. J. Virol. **78:**6967–6973.
36. **Yamayoshi, S., et al.** 2008. Ebola virus matrix protein VP40 uses the COPII transport system for its intracellular transport. Cell Host Microbe **3:**168–177.
37. **Yamayoshi, S., et al.** 2009. Scavenger receptor B2 is a cellular receptor for enterovirus 71. Nat. Med. **15:**798–801.
38. **Yan, J. J., J. R. Wang, C. C. Liu, H. B. Yang, and I. J. Su.** 2000. An outbreak of enterovirus 71 infection in Taiwan 1998: a comprehensive pathological, virological, and molecular study on a case of fulminant encephalitis. J. Clin. Virol. **17:**13–22.
39. **Yang, B., H. Chuang, and K. D. Yang.** 2009. Sialylated glycans as receptor and inhibitor of enterovirus 71 infection to DLD-1 intestinal cells. Virol. J. **6:**141.
40. **Yang, F., et al.** 2009. Enterovirus 71 outbreak in the People's Republic of China in 2008. J. Clin. Microbiol. **47:**2351–2352.